NY-14-040

The Formation and Runoff of Condensate on a Vertical Glass Surface

Vivek Kansal, PEng

John L. Wright, PhD, PEng
Member ASHRAE

Michael R. Collins
Member ASHRAE

ABSTRACT

An experimental study of condensate formation and runoff was performed by exposing a sheet of glass, cooled at its bottom edge, to an enclosure with a controlled environment. This arrangement mimics the indoor glass surface at the bottom edge of a window when the window is exposed to a cold, outdoor environment. The air in the enclosure was maintained at a constant dry-bulb temperature (T_{db} *= 22.1°C* [T_{db} *= 71.8°F]) and constant relative humidity (RH = 30%, 35%, 40%, 45%, or 50%) during individual experiments. It was found that the time until initial runoff,* t_{ir}*, decreased with increasing RH, and* t_{ir} *was sensitive to RH at low RH, but insensitive to RH at high RH. At first, condensate runoff occurred near the bottom of the glass and left one to believe that the remaining condensate was at steady state. But over a 16-hour period, it was found that the condensate runoff front, in every case, progressed upward to include the entire condensate area. The speed of the condensate runoff front increased with RH, and was less sensitive to RH at low RH. Measurement results were used to produce a summary plot showing runoff front position as a function of glass surface temperature and RH. This chart can be used to predict* t_{ir} *and runoff front progression at the bottom edge of any window if the surface temperature profile is known.*

BACKGROUND – MOLD IN BUILDINGS

Mold (fungus) growth within a building envelope can be hazardous. Through touch or inhalation, the effects of mold can vary from mild allergic reactions to fatality. Mold growth in the building envelope occurs when moisture is present on common building materials, such as house dust, wallpaper, textiles, wood, paint, gypsum board, fiber board, and glue (Dalton 2004; IOM 2004). Symptoms of mold include headaches, sneezing, eye and skin irritation, runny nose, difficulty breathing, and asthma (EPA 2002). In 1994, Dr. David Sherris of the Mayo Clinic determined mold to be the cause of chronic sinus infections in 93% of his 210 test patients (Underwood 2000). Studies at the Lawrence Berkeley National Laboratory concluded with statistical significance that mold and building dampness are associated with a 30% to 80% increase in respiratory and asthma related problems (Fisk et al. 2006). More serious health effects caused by repeated contact with mold include hypersensitivity pneumonitis, pulmonary hemorrhaging, cancer of the liver, brain hemorrhaging, and narcosis; all are potentially fatal (EPA 2001; Dearborn et al. 1999; Barrett 2000; Wang et al. 2001). These effects are caused when mycotoxins are found in the mold.

Mold growth potential is defined as the minimum moisture required for microbial growth in terms of "water activity." Water activity, a_w, is defined as the ratio of the moisture content, by mass, of the material in question to the moisture content of the same material when it is saturated. When a material is fully saturated, $a_w = 1$, it is in equilibrium with air at relative humidity (RH) of 100% (IOM 2004). *Penicillium* and *Aspergillus* can start growing at $a_w = 0.76$, while *Cladosporium* and *S. chartarum* can start growing at $a_w = 0.83$ and 0.91, respectively (Grant et al. 1989). Lstibrurek (2002) asserts that elevated RH at a surface, 70% or higher, can lead to problems with mold, corrosion, decay, and other moisture related deterioration. It is important to recognize that RH will be higher near a cooled surface even though the absolute humidity may be constant throughout the indoor space. If a surface is cooled to the extent that condensation forms, then RH = 100% is the condition adjacent to that surface.

Vivek Kansal is a service manager at Automated Logic Corp., Concord, ON, Canada. **John L. Wright** is a professor and **Michael R. Collins** is an associate professor in the Department of Mechanical and Mechatronics Engineering, University of Waterloo, ON, Canada.

Mold growth also requires nutrients. Suitable nutrients include carbohydrates, proteins, lipids, or even non-biologic compounds (IOM 2004). Such nutrients are usually found in house dust, wallpapers, textiles, wood, paints, gypsum board, fiber board, and glue (Dalton 2004; IOM 2004). Once present, the rate of mold growth varies depending on mold type and environmental conditions. Some types of micro organisms can multiply from one cell to one billion in 18 hours (White and Kuehl 2002). In a study of penicillium on wallpaper, mold growth was observed in as little as 5 hours (Pasanen et al. 1992).

The final necessity for mold growth is a suitable temperature. Mold thrives at temperatures of 4°C to 38°C (40°F to 100°F) (Post 1999). The typical house will include many indoor surfaces within this temperature range, so temperature is not a limiting factor.

To find potential mold growth locations, it is best to look for sitting water on building materials. Main sources of water in the household are moisture from a shower in a bathroom, cooking, a leaky pipe, condensate from cold water pipes, or water from sinks and tubs. Another obvious source is a window. Condensation that forms on a window, under certain circumstances, may run off the window and pool at the window sill or on the window frame. If the situation persists, water may flow into the wall below the window and seep into the insulation.

Mold growth on or around window frames has been well documented. A study of 200 houses with water incursions in Texas cited window frames as one of the locations for surface fungal growth (Kuhn 2005). Morrell (2002) highlighted the types of mold typically found on window frames in a study of wood-based construction. McNeel and Kreutzer (1996) also identified household molds found on window sills. Grant et al. (1989) stated gloss paint on window joinery supports mold growth. Surveys conducted by Statistics Canada for Natural Resources Canada found that 42% of houses surveyed reported window condensation and cited it as a problem that could lead to mold growth (NRCan 2005). The US Environmental Protection Agency lists prevention of condensation on windows as a way to reduce the risk of mold in the building envelope (EPA 2002). Condensation on windows has been cited, in numerous references, as the cause of mold growth on window glass and frames (Bailey and Hall 2006; Godish 2002).

The National Fenestration Rating Council (NFRC), Canadian Standards Association (CSA), and American Architectural Manufacturers Association (AAMA) have developed methods to evaluate the "condensation resistance" of a window. These methods, documented in the NFRC 500, CSA A440.2, and AAMA 1503 standards, each provide a measure of the severity of condensate formation. Although it is important to know whether condensation will form on a window surface, it is equally important to predict whether condensate runoff will occur. Condensation that forms on a window, but does not run off to pool on the sill or collect in the walls, presents a much smaller health risk and represents little potential for damage to the building.

BACKGROUND—THE MECHANICS OF CONDENSATION

The Bottom Edge

If the outdoor temperature is sufficiently low, condensation will occur on the indoor surfaces of any window. Condensate will form in any location where the surface temperature falls below the dew-point temperature, T_{dp}, of the indoor air. Condensation occurs most readily at the perimeter of the view area (i.e., at the sightline). This is a sign that condensation is caused by edge-seal conduction and the edge-seal is widely, and correctly, recognized as a thermal short-circuit (e.g., Wright and Sullivan 1989; Reilly 1994; Wright et al. 1994). Even modern thermally improved edge-seals represent a thermal short circuit.

It is also known that condensate forms most readily at the bottom edge of the view area. This happens for several reasons, but primarily because fill gas motion cools the bottom of the indoor glass. In winter, at night, fill gas flows upward, adjacent to the warm indoor glass, and downward near the cold outdoor glass. The descending gas becomes progressively colder. At the bottom of the cavity, the cold fill gas turns and, as it starts its ascent, it cools the indoor glass. The result is that the bottom edge of the indoor glass is preferentially cooled by the fill gas. This bottom-edge heat transfer phenomenon has been studied and confirmed by experiment and analysis (Wright and Sullivan 1995; Sullivan et al. 1996; Curcija and Goss 1998; Wright 1998; Wright and McGowan 2003). The current study of condensate formation and runoff is focused on the bottom edge-glass section of the window, the location where condensate most readily forms and where the runoff/accumulation of condensate is most prevalent.

Condensate Formation and Runoff

When condensate forms on window glass, it is easy to tell if runoff has occurred. The pool of water at the sill provides clear evidence. Figure 1 shows a photograph of bottom-edge condensate during cold weather. The condensate itself consistently forms as discrete droplets, but the band of edge-glass condensate is generally comprised of two sections. In Figure 1 evidence of condensate runoff can be seen in the lower section. When runoff takes place, it leaves tracks and patches behind that are temporarily free of droplets. In the upper section, various droplet sizes can be seen, but no runoff is observed. Progressing upward, the droplets decrease in size and become small enough to appear as a thin uniform layer or mist at the top edge of the condensate band.

The differences from bottom to top of the condensate band are caused by the difference in glass surface temperature. The glass is coldest at the sightline, and gets progressively warmer toward the center-glass section of the window. The edge of the condensate band corresponds to the location where the glass temperature is equal to T_{dp}. The rate at which condensate forms is greater on colder surfaces, as might be expected, and this difference gives rise to the variety of appearances that are observed across the condensate band.

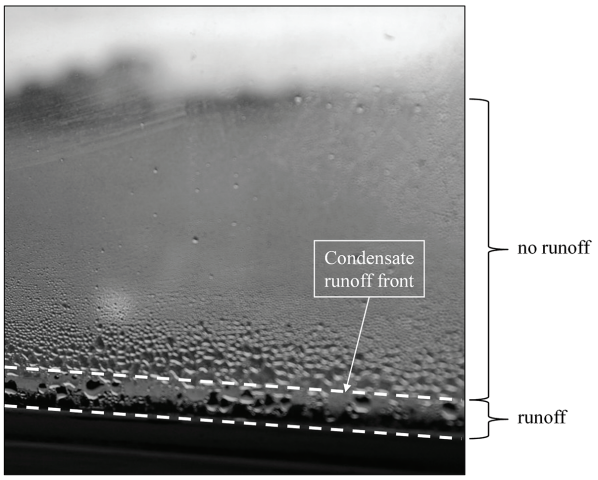

Figure 1 *Condensation at the bottom edge of a window.*

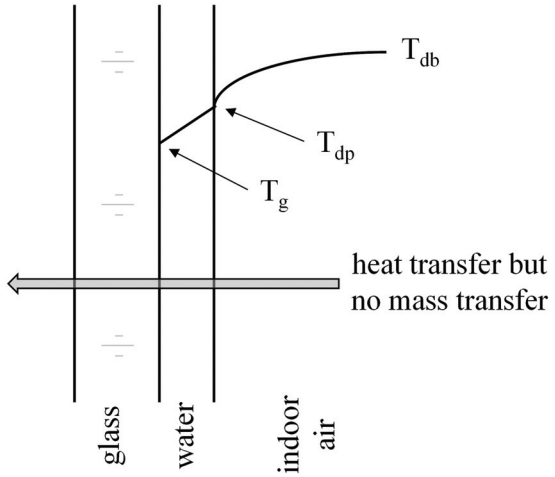

Figure 2 *Temperature profile through condensate film, at steady state, without runoff.*

Condensation at Steady State

It is impossible to tell from the image in Figure 1 whether the condensation process in the upper section is at steady state or if, over a longer period of time, condensation will also cause runoff from the upper band. In other words, when condensate appears on a cold window, it is hard to tell if the process is at a steady state or in transition to steady state because change is so slow. An observer could easily get the impression that a fine layer or mist of condensate will remain in place indefinitely and no runoff will occur. In order for this to happen, the formation of condensate (i.e., the mass transfer) must stop, and this implies that the temperature of the exposed liquid-air interface is equal to T_{dp}.

To better understand this concept, consider a fictitious situation in which the condensate exists as a uniform layer, on a cooled surface, as shown in Figure 2. Let us assume that this liquid layer is stationary. The condensate layer will possess some finite thermal resistance, resulting in a temperature rise from the solid surface to the exposed liquid surface. A thick layer has more thermal resistance than a thin layer, so if the liquid layer is thin, condensation will continue and the condensate layer will thicken until the temperature of the liquid/air interface rises to T_{dp}. When this condition is reached, condensation stops. In this situation, steady state exists and there will be no mass transfer even though heat transfer remains.

The previous paragraph describes a situation that is unrealistic. A liquid film would not be stationary and, more to the point, it is known that the condensate clings to the glass in the form of droplets. Even a very fine condensate layer that appears to be uniform consists of very small droplets. Droplets on the glass surface grow and coalesce as condensation progresses. These droplets comprise an irregular terrain of different water thickness, as shown in Figure 3, and different amounts of thermal resistance in different locations. It is possible that the surface temperature of some large droplets will rise as high as T_{dp}, but it might be anticipated that condensation will continue in the colder locations closer to the glass. If so, it can also be expected that the smaller droplets will grow and coalesce with adjacent droplets, eventually producing droplets that are sufficiently large to break free and run down the surface. This study was undertaken, in part, to see if this sequence of events proceeds as described.

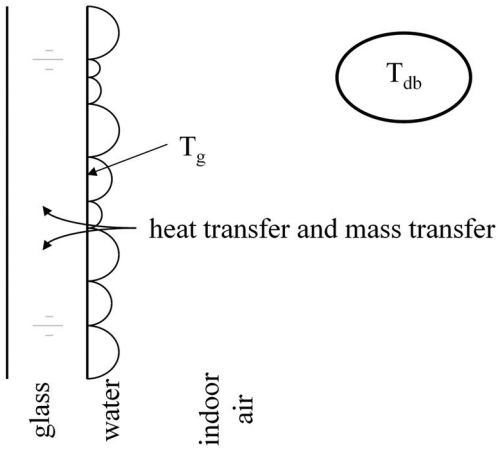

Figure 3 *Heat transfer through droplet condensate.*

OBJECTIVE

The general objective of this study was to obtain information about the way in which water vapor condenses, accumulates, and runs from a cooled vertical sheet of glass. More specifically, information was sought regarding the conditions (dry-bulb temperature, relative humidity, surface temperature) under which condensation will or will not run and, if it does, where and when the runoff occurs.

In light of the considerations discussed above, the objectives of this study can be refined to include the following three questions:

1. Can a layer of water droplets exist indefinitely on a glass surface without running (i.e., at steady state with no further condensation)?
2. If so, under what conditions does this occur?
3. If not, how long does it take before runoff occurs, and how does the condensate runoff front progress with respect to time?

THE APPARATUS

A series of experiments was undertaken to visually inspect condensate formation and runoff. A sheet of clean glass on one wall of an enclosure was cooled and exposed to air at controlled levels of RH and dry-bulb temperature, T_{db}. Observations were made to determine if and when runoff occurs as condensate forms on the glass surface. Multiple experiments were conducted. The condition inside the enclosure was controlled at T_{db} = 22.1°C (T_{db} = 71.8°F) and at one of five RH values; RH = 30%, 35%, 40%, 45%, or 50%. Tests spanned 950 minutes, typical of a long winter night. The longest night in Waterloo, Ontario, Canada (latitude 43.3°N), at the winter solstice, lasts 915 minutes.

The enclosure was also designed such that the heat transfer at the exposed glass surface, both convective and longwave, would resemble the heat transfer that exists at the surface of a window exposed to a large indoor space. Natural convection is of interest in this case. ASHRAE (2005) lists indoor surface heat-transfer coefficients for this situation, for double-glazed windows, over a range of about h = 6.8 W/m^2·K to h = 7.7 W/m^2·K (1.2 to 1.36 Btu/h·ft^2·°F). Knowing that glass has an emissivity of ε = 0.84, the longwave radiant portion of h is approximately h_r = 5 W/m^2·K (0.9 Btu/h·ft^2·°F). Thus, the convective heat-transfer coefficient of interest falls in the range of about h_c = 1.8 W/m^2·K to h_c = 2.7 W/m^2·K (0.3 to 0.5 Btu/h·ft^2·°F).

The apparatus consisted primarily of a cooled vertical sheet of glass exposed to a conditioned, enclosed space. The back surface of the glass was bonded to an aluminum plate that was cooled by a manifold block attached to the bottom edge of the backing plate (see Figures 4 and 5). A flow of coolant (a glycol mixture) was supplied to the manifold block by a constant temperature bath. The coolant was routed through the manifold in alternating directions to maintain a uniform temperature along the length of the manifold.

The heat-transfer coefficients at the exposed glass surface were not measured. Instead, two-dimensional (2-D) computational fluid dynamic (CFD) calculations were used to aid the design process. Initially, a simple four-surface enclosure was analyzed. The enclosure walls were each isothermal, with three hot walls and one vertical cold wall. Simulation parameters (e.g., grid size, convergence criteria, etc.) were found that produced close agreement between CFD results and an empirical solution for a laminar boundary layer on a free-standing vertical plate.

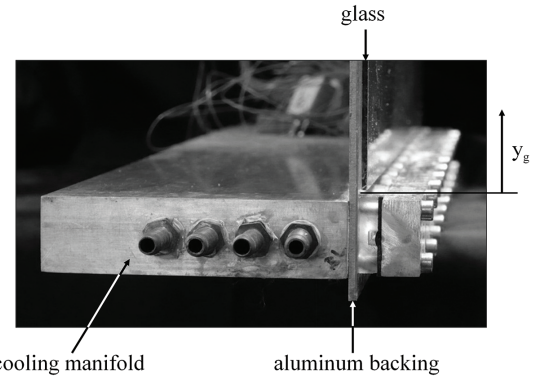

Figure 4 *Cooling manifold and bottom section of glass test surface.*

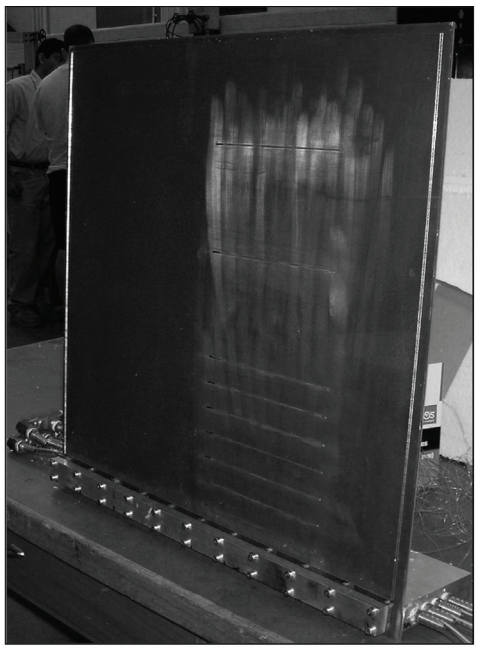

Figure 5 *Face view of glass test surface showing aluminum back plate, thermocouple locations, and bottom-mounted cooling manifold.*

Then more detail was added to the CFD model. These details included glass, aluminum backing plate, and bottom-edge cooling manifold (i.e., surface of interest no longer isothermal). A compromise was sought that would allow the apparatus to be tall enough for h_c to be in the range of interest (i.e., sufficiently low, in or near the range of 1.8 to 2.7 W/m^2·K (0.3 to 0.5 Btu/h·ft^2·°F, discussed above), and for h_c to be reasonably uniform in the location of interest, but small enough for a table-top experiment. It was determined that a vertical 500 mm (19.7 in.) sheet of glass on one wall of the enclosure would experience an average convective heat

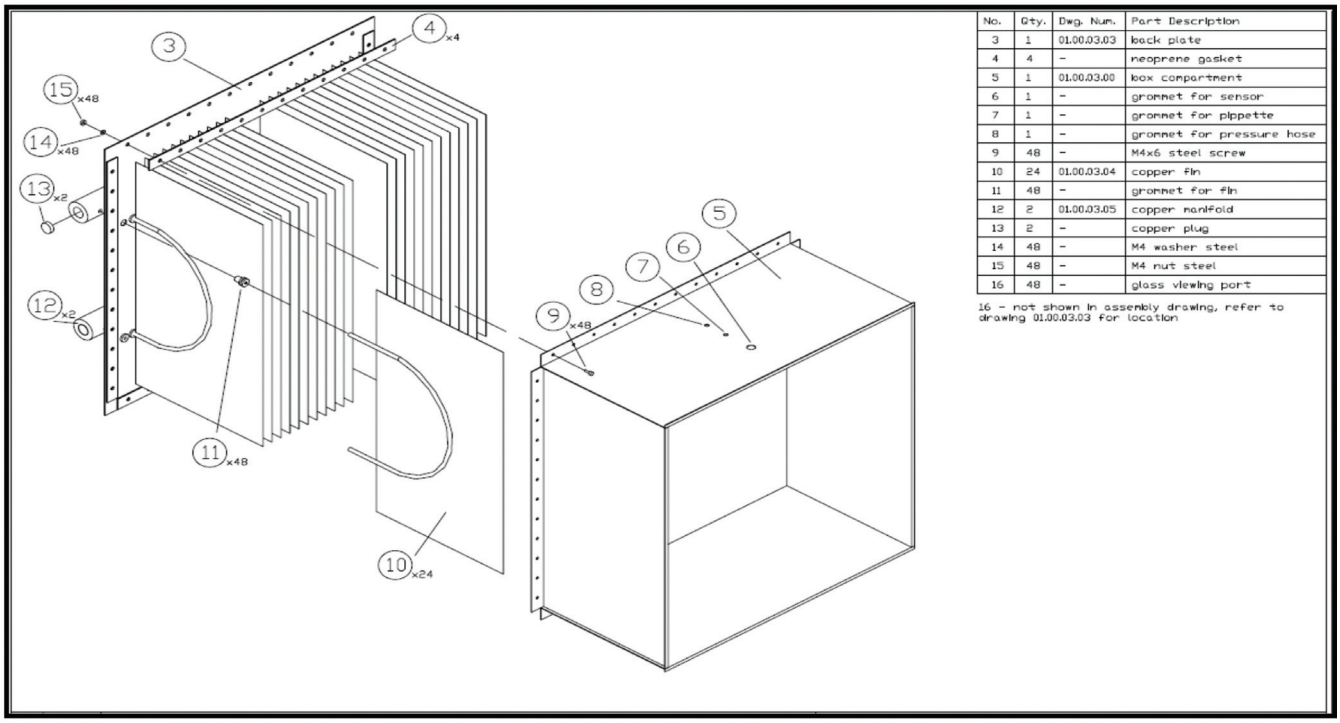

No.	Qty.	Dwg. Num.	Part Description
3	1	01.00.03.03	back plate
4	4	–	neoprene gasket
5	1	01.00.03.00	box compartment
6	1	–	grommet for sensor
7	1	–	grommet for pippette
8	1	–	grommet for pressure hose
9	48	–	M4x6 steel screw
10	24	01.00.03.04	copper fin
11	48	–	grommet for fin
12	2	01.00.03.05	copper manifold
13	2	–	copper plug
14	48	–	M4 washer steel
15	48	–	M4 nut steel
16	48	–	glass viewing port

16 - not shown in assembly drawing, refer to drawing 01.00.03.03 for location

Figure 6 *Assembly drawing of back/side walls of enclosure, fin array, and heating manifolds.*

transfer coefficient of 2.7 W/m^2·K (0.5 Btu/h·ft^2·°F) over its full height, but in the area of greatest interest, the bottom 120 mm (4.7 in.) of the glass, h_c was estimated to range from 1.7 to 2.3 W/m^2·K (0.3 to 0.4 Btu/h·ft^2·°F).

It was also noted that the choice of vertical dimension, 500 mm (19.7 in.), would preclude a transition to turbulence, and the associated complexity/uncertainty, in the boundary layer near the bottom of the glass.

The CFD calculations also indicated that the air in the center of the enclosure would be unacceptably stratified. Instead of using a fan to mix the air, a large number of vertical copper fins were installed in the enclosure to heat the air while minimizing stratification. Figure 6 shows the fin arrangement. Figure 6 is intended to show only qualitative information about the fin arrangement. Quantitative detail, including the labels that are illegible in Figure 6, can be found in Kansal (2006). The enclosure was sized to be 500 mm (19.7 in.) deep (perpendicular to the glass) in order to install sufficient fin area. The large-finned heating area provides two additional benefits. The fins heat the air in the bulk of the enclosure to a temperature very close to the wall (i.e., fin) temperature, and the fin geometry provides the glass surface with a longwave radiant environment that is similar to a large room (i.e., almost black). The fins were positioned at a sufficient distance so that they would not interfere with the boundary layer at the glass surface. Additional detail regarding the enclosure analysis can be found in Kansal (2006).

The array of copper fins, fed by a constant temperature bath, was used to control the dry-bulb temperature inside the enclosure. During each experiment, T_{db} and RH were simultaneously monitored using a Vaisala RH1000 sensor (Vaisala 2005). The stated accuracy of the temperature measurement is ±0.2°C (±0.36°F). A pipette was used to add water and control the RH. A small electrical heater (1 Watt) was used to evaporate water droplets as they were added to the enclosure. A built-in control feature of the RH1000 sensor regulated the addition of water droplets. The RH1000 system has a stated accuracy of about 1% to 1.5% RH, and the required enclosure RH was generally maintained within a 1% RH span (e.g., RH = (50±1)%) as water was removed by means of condensation and periodically replenished by droplets.

The temperature profile of the glass surface was not uniform. The glass was coldest at its bottom edge, similar to the glass in a window. Temperature along the glass surface was monitored using thermocouples bonded into slots in the aluminum backing plate and in contact with the unexposed surface of the glass. The thermocouple slots were positioned to eliminate lead losses. The leads of nine thermocouples can be seen in Figure 5. The uncertainty associated with these thermocouples was estimated to be ±0.2°C (±0.36°F). The temperature change through the thickness of the glass was estimated to be ±0.2°C (±0.36°F) at most, so thermocouple readings are presented as glass surface temperatures without adjustment.

The choice to cool the glass surface from its bottom edge is convenient because this arrangement resembles the bottom edge-glass area of a window installed in a house. There is also a more subtle benefit. The cold bottom edge arrangement allows for the observation of condensate formation on surfaces at various temperatures during a single test. As condensate accumulates at any given location and eventually runs down the glass, it only alters (i.e., clears) the surface in locations where condensate has already begun to run. Condensate runoff does not interfere with higher locations where condensate is still accumulating and being observed.

MASS-TRANSFER COEFFICIENT

The condensation process entails the migration of water vapor from the bulk room air to the glass surface, where it changes phase and gives up its latent energy. This mass transfer is driven by the water vapor concentration gradient. In a similar way, convective heat transfer is driven by the temperature gradient. In fact, convective heat transfer in air and mass transfer of water vapor in air are very similar processes. In both cases, the quantity of interest, mass or energy, is transported by a combination of advection and diffusion. The similarity with respect to advection is clear because both processes are subject to the same velocity field. Similarity with respect to diffusion (conduction is the diffusion component of the heat-transfer process) can readily be shown to exist because of the specific set of transport properties at play (e.g., thermal conductivity, coefficient for diffusion of water vapor in air). More formally, the similarity of the two processes can be demonstrated because the Prandtl number and Schmidt number of the moist air mixture do not differ appreciably. Consequently, similarity theory can be used to calculate h_c if the corresponding mass-transfer coefficient is known, and vice-versa.

The point of importance is that the heat-transfer and mass-transfer coefficients are linked. One will change in the same way that the other changes, for example, with respect to location. In the experiments comprising this study, an effort was made to establish a heat-transfer coefficient, h_c, that realistically represents natural convection. Accordingly, the mass-transfer coefficient will also be realistic and representative of natural convection at the glass surface.

PROCEDURE

To establish a "time-zero" (t = 0) for each experiment, desiccant was used to dry the enclosure between experiments. The surface of the glass was cleaned before each experiment, and a consistent start-up procedure was employed. Prior to each experiment, the enclosure was brought to RH = 25% and T_{db} = 22.2°C (T_{db} = 72°F). This combination was chosen because the dew-point temperature exceeds the temperature of the coldest portion of the glass, ensuring that no condensation could form prior to t = 0. At t = 0, RH was quickly raised to the desired value.

A number of experiments were completed. The constant temperature bath settings remained unaltered for the complete set of tests in order to maintain a consistent cooling manifold temperature (near 0°C) and T_{db} = 22.1°C (T_{db} = 71.8°F) in the enclosure. The bottom edge of the glass was observed through a small glass view port in the back wall of the enclosure. A similar port in the side wall was used, as needed, to illuminate the glass surface. The width of the condensate band and the location of condensate runoff was judged by eye, using the thermocouple locations as a distance scale. Photographs were also taken through the view port but, because of the confined view-angle between fins and limited available light, the photographs did not provide as much detail/reliability as direct visual observation. A more complete data set, with a full set of images, can be found in Kansal (2006).

Measurements of T_{db}, RH, and glass temperature were made during each experiment.

RESULTS—GENERAL OBSERVATIONS

Observation showed that, over time, a steady-state condition without runoff does not occur. In all cases, runoff was observed and the runoff front (see Figure 1) progressed fully to the top of the condensate band. Condensation was always in the form of droplets. At first, a fine mist consisting of very small droplets formed on the glass surface, and individual droplets were difficult to resolve by eye. As time progressed, small droplets coalesced and formed larger droplets. In turn, the larger droplets coalesced and formed still larger droplets. This process continued until droplets became large and heavy enough to overcome surface tension and run down the glass.

As expected, droplet growth was faster at the lower, colder portion of the glass, and a range of droplet sizes could be seen, from large droplets and runoff at the bottom of the glass, to small droplets in the intermediate section and mist near the dew-point line.

GLASS SURFACE TEMPERATURE

Thermocouple readings were taken to record the glass temperature at the beginning and end of each experiment. The recorded values did not vary appreciably between runs or between the beginning and end of an individual run. The range of temperatures measured at any location, over the course of all experiments, spanned 0.7°C (1.26°F), at most. The average temperatures for all readings are shown in Figure 7, where glass temperature, T_g, is shown on the horizontal axis, and distance from the bottom edge of the glass, y_g, is shown on the vertical axis. Each point on the plot corresponds to a thermocouple location along the glass surface. The best-fit curve, shown in Figure 7, is given by Equation 1, and this curve is used to represent the glass surface temperature in subsequent operations.

$$y = 7.397 + 1.393245x + 2.38795x^2 - 0.20785x^3 + 0.007436x^4 \quad (1)$$

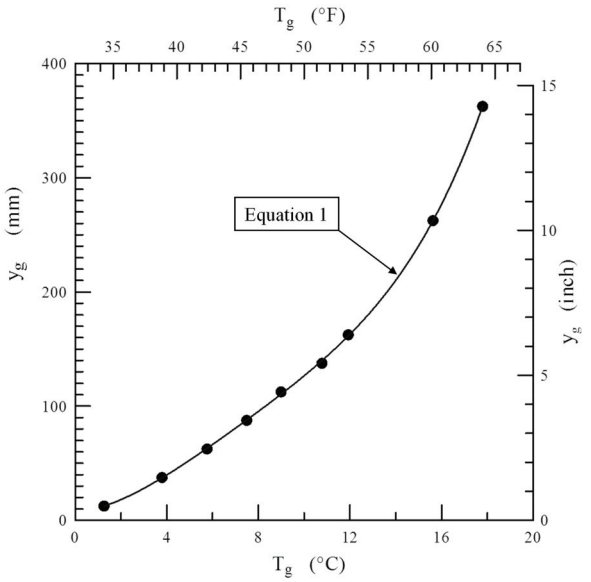

Figure 7 *Glass temperature (horizontal axis) versus* y_g *(vertical axis) measurements and curve fit.*

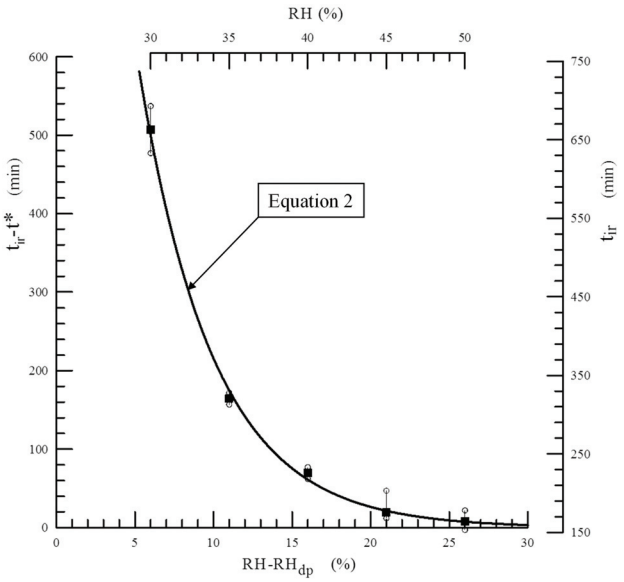

Figure 8 *Time to initial runoff versus RH.*

where

x = T_g, °C
x = $(T_g - 32) / 1.8$, °F
y = y_g, mm
y = $y_g / 25.4$, in.
R^2 = 0.9999 (coefficient of determination)

TIME OF INITIAL RUNOFF

Visual observations were used to estimate the time of initial condensate runoff, t_{ir}, during each experiment. Runoff presents itself as discrete occurrences where individual droplets run down the glass, so this observation of t_{ir} corresponds to one or more such occurrences in the relatively narrow area where the glass could be observed between the fins. The results are shown in Figure 8, where the scale for t_{ir} is shown on the right, and the RH scale is shown above the chart.

The data shown in Figure 8 were plotted to show the range of t_{ir} obtained from multiple experiments. Experiments were repeated to obtain a sense of accuracy for the visual measurement. For example, three experiments were conducted at RH = 50%, and initial runoff occurred between t = 150 minutes and t = 165 minutes for two experiments, and between t = 160 minutes and t = 175 minutes for the third experiment. The low open symbol is at t = 150 minutes, the high open symbol is at t = 175 minutes, and the darkened symbol at t_{ir} = 160.8 minutes marks the average of 157.5, 157.5, and 167.5 minutes.

The bottom horizontal axis in Figure 8, (RH – RH_{dp}), is of interest because RH_{dp} is the RH level at which T_{dp} = 0°C (T_{dp} = 32°F). Condensate that forms on glass that is colder than 0°C (T_{dp} = 32°F) can be expected to freeze before runoff occurs, so it might also be expected that RH_{dp} acts as a vertical asymptote, and the data shown in Figure 8 support this idea. Experiments were completed with T_{db} = 21.1°C (T_{db} = 71.8°F), so RH_{dp} = 24% for the given enclosure.

It can be seen that RH has little influence on t_{ir} for cases with RH > 45%, but t_{ir} is strongly influenced by RH at low RH levels. In all cases, runoff does occur within a 16-hour period. It can be seen in Figure 8 that the data at high RH appear to approach a horizontal asymptote near t = 150 minutes. The data closely match an exponential curve fit, with the residual minimized (R^2 = 0.997) when the horizontal asymptote is set at t^* = 153 minutes. This curve fit, given by Equation 2, is also shown in Figure 8. Note that the asymptotes align with the left axis and bottom axis, ($t_{ir} - t^*$) and (RH – RH_{dp}), respectively.

$$y = 1760.7e^{-0.21x} \quad (2)$$

where

x = $RH - RH_{dp}$, %
RH_{dp} = 24%
y = $t_{ir} - t^*$, min
t^* = 153 min
R^2 = 0.997 (coefficient of determination)

RUNOFF FRONT SPEED

Visual observations were also used to estimate the speed of the runoff front, V_{rf}. A plot showing V_{rf} versus RH – RH_{dp} is shown in Figure 9. The value plotted is the rate

observed shortly after the front began to move. Figure 9 shows an increase in V_{rf} as RH is increased. This is expected as the higher RH imposes a higher driving potential for mass transfer. This, in turn, results in a faster progression through the droplet formation process and faster runoff front progression. Estimated runoff speeds were obtained by visual observation, and these observations were often 30 to 60 minutes apart. Hence, the margin of error in the V_{rf} values is significant. It should be noted that the runoff front did not move appreciably over 950 min at RH = 30%. It is very much a possibility that the front did move, but so slowly that it was difficult to notice.

A very simple curve fit was chosen to represent the data shown in Figure 9, largely because of the uncertainty attached to the measurement of V_{rf}. Two considerations were used to select the format of the curve fit. First, V_{rf} must be zero at RH_{dp}, as condensation, let alone runoff, would not occur with RH < RH_{dp}. Second, the slope of the curve was set to zero, $\partial V_{rf}/\partial \text{RH} = 0$, at RH = RH_{dp} because, in the absence of condensation, the slope must be zero at $RH < RH_{dp}$, and a discontinuity is not expected at RH – $RH_{dp} = 0$. It is not necessarily clear that there is no discontinuity at this location, but the measurements do not support the idea of a discontinuity. The curve shown in Figure 9 is given by Equation 3. The coefficients used in Equation 3 were chosen by (a) placing a higher priority on matching data in the RH = 30% to RH = 40% range because lower RH is more common and (b) recognizing that the V_{rf} = 0 data point at RH = 30% is subject to error because of the difficulty of measuring the location and speed of a condensate runoff front in a narrow condensate band.

$$y = \frac{1}{3000}x^2 \tag{3}$$

x = $RH - RH_{dp}$, %
RH_{dp} = 24%
y = V_{rf}, mm/min

GRAPHICAL SUMMARY

The interrelation between RH, T_g, t_{ir}, and V_{rf} can be summarized in a single chart for situations with $T_{dp} \approx 22.1$°C (T_{dp} = 71.8°F). See Figure 10. The curved line in the upper-left portion of Figure 10 shows T_g as a function of y_g for the glass surface used in the experimental work. The T_g axis is shown above the curve, and the y_g axis is on the left. The T_g versus y_g curve is identical to the curve shown in Figure 7 (i.e., Equation 1).

The lines plotted in the lower right portion of Figure 10 show t_{ir} as a function of y_g. The t_{ir} axis is at the bottom of the chart. Each t_{ir} versus y_g relation corresponds to a specific RH value, as shown. The leftmost end of each sloped line segment corresponds to the time (Equation 2) and location (y_g = 25 mm [0.98 in.] for RH = 30%, y_g=38 mm [1.5 in.] otherwise) that runoff was first observed, and the slope itself is V_{rf}, given by Equation 3. The knee between the line segments corresponds to T_{dp} for each corresponding RH value. At T_{db} = 22.1°C (T_{db} = 71.8°F), T_{dp} = 3.74°C, 5.96°C, 7.85°C, 9.74°C, and 11.2°C (38.7°F, 42.7°F, 46.1°F, 49.5°F, and 52.2°F) for RH = 30%, 35%, 40%, 45%, and 50%, respectively. If $T_g > T_{dp}$ in a given location, no condensate will form, so $t_{ir} \to \infty$ at that location.

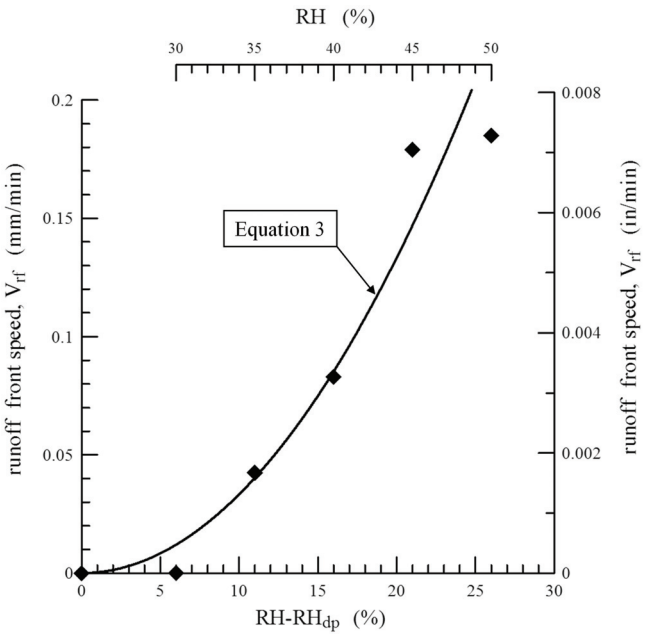

Figure 9 *Speed of condensate runoff front versus relative humidity.*

All of the information presented in Figure 10 pertains to observations made in the laboratory, but this chart can be used to estimate t_{ir} for any window if the surface temperature profile of the glass is known. This conversion relies on the assumption that t_{ir} is a function of T_g alone (for a given RH). This assumption is supported by the idea that runoff only disturbs the condensate in locations where runoff has already been initiated—glass below the location of interest. This is the situation at the bottom edge-glass area of a window installed in a house. The influence of the runoff front does not extend to higher locations of the glass surface, by definition.

An example of the laboratory-to-window conversion is shown by the dotted lines in Figure 10. Start at the top of the chart. In this case, it is known that the glass temperature at a specific location near the bottom of a particular window is T_g = 7°C (44.6°F). The T_g versus y_g curve can be used to find the location where the glass was at this temperature in the experiment, $y_g \approx 80$ mm (3.1 in.) in this case. At this stage, the conversion has been made from window to experiment. Then, working to the right it can be seen that $t_{ir} \approx$ 720 min at RH = 40%, but neither condensate nor runoff should be expected if RH is less than about 38%. It should be emphasized that y_g of the window and y_g of the experiment may differ appreciably. Remember, the glass used in the experiment was bonded to an aluminum plate to inten-

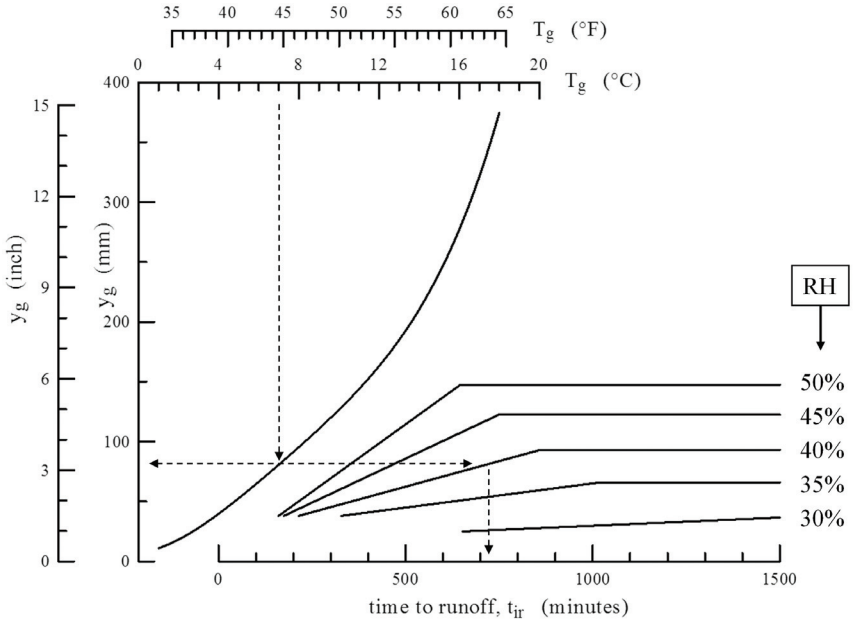

Figure 10 *Time and location of initial runoff versus surface temperature and relative humidity (based on Equations 1, 2, 3, and* T_{db} *= 22.1°C [71.78°F]).*

tionally decrease the temperature gradient along the glass and widen the condensate band. The connection between the two locations, window versus experiment, is that they have the same glass temperature.

In addition to estimating t_{ir}, it is possible to estimate V_{rf} for some window of interest. The slope of the line segment shown in Figure 10 represents V_{rf} for the experiment, but this particular value does not apply to window surfaces in general. As noted above, the temperature profile across the edge-glass section of a window installed in a house will probably differ appreciably from the profile used in the experimental work. In fact, one window will differ from another window. Nonetheless, V_{rf} can be estimated in a two-step process. First, choose one value of y_g, say $y_{g,1}$, near the bottom edge of the condensate band and, starting with the corresponding glass temperature, work through Figure 10 to find t_{ir} for that location, say, $t_{ir,1}$. Second, use Figure 10 to repeat the process, starting with a known glass temperature corresponding to $y_{g,2}$, and find $t_{ir,2}$. Equation 4 can then be used to estimate the speed of the runoff front for the window of interest, $V_{rf,w}$. The necessary correction, to adjust for the difference between temperature profiles, is an implicit component of this procedure.

$$V_{rf,w} = \frac{y_{g,2} - y_{g,1}}{t_{ir,2} - t_{ir,1}} \tag{4}$$

It is also possible to work backward through Figure 10 to answer other types of questions. For example, "What is the lowest glass temperature, at a given RH, required to prevent condensate runoff for a certain amount of time?" Or, "What is the maximum RH that can be used while avoiding runoff at a particular location and a particular time?"

CONCLUDING REMARKS

The main purpose of this set of experiments was to determine if, and under what conditions, condensation would produce runoff from the bottom edge-glass area of a window exposed to a cold outdoor environment. Clearly, condensate runoff is undesirable with respect to the possibilities of both mold growth and direct material damage but, to be clear, this work cannot be used to comment on the likelihood of mold or damage. This connection warrants further research but is well beyond the scope of the present study.

Experiments were conducted with the temperature of the conditioned space at T_{db} = 22.1°C (T_{db} = 71.8°F) and RH = 30%, 35%, 40%, 45%, and 50%. The surface temperature of the glass, T_g, was controlled to be consistent from one experiment to the next. The bottom edge of the glass was cooled to the extent that condensation was observed in every case. Condensate runoff was also observed in every case, initially at the bottom edge of the glass, and the condensate runoff front progressed upward to the top of the condensate band in every case.

The initial runoff time, t_{ir}, was noted by visual observation in each experiment. It was determined that t_{ir} decreases with increased RH, is sensitive to RH at low RH, but insensitive to RH at high RH. The relationship can be seen in Figure 8.

The speed of the runoff front, V_{rf}, was also noted visually. The runoff front moves more quickly as RH is increased and V_{rf} is insensitive to RH at low RH, but sensitive to RH at high RH. The relationship can be seen in Figure 9. The formation of condensate at RH = 30% was particularly slow, and was confined to a small area, so V_{rf} could not be determined reliably for this situation.

A summary chart has been devised to show the interrelation between RH, T_g, t_{ir}, and V_{rf}. See Figure 10. This chart can be used to estimate t_{ir} and V_{rf} for the bottom edge-glass area of any window, as long as the surface temperature of the glass is known.

This study represents the first time that experiments have been undertaken to explicitly study the formation and runoff of condensate on a glass window surface. A number of interesting observations have been made. However, even though an effort was made to ensure accuracy, repeatability, and relevance, it would be useful to confirm these observations independently. This idea can be emphasized by pointing out that many of the measurements rely on visual observation using an apparatus with which it was difficult to see and/or photograph the test surface. There is value in undertaking a similar study using a full-size window exposed to a large enclosure (i.e., a room). The full-scale version of the experiment would be less difficult to build, would ensure realistic and more uniform heat-/mass-transfer coefficients, and would provide better visual access—possibly providing better measurement of t_{ir} and V_{rf} at low RH. In a more detailed experiment, it might also be possible to measure the flow rate of condensate that runs to the window sill. A more detailed experiment might also resolve V_{rf} at different stages of progression, showing that the sloped line segments in Figure 10 should actually be curved, merging more smoothly with the horizontal line segments. Nonetheless, the current study provides useful insight, including qualitative and quantitative observations that are of value for the engineering of modern window systems.

ACKNOWLEDGMENTS

This research was supported by the Canadian Window & Door Manufacturers Association. Their support is gratefully acknowledged.

REFERENCES

ASHRAE. 2005 ASHRAE Handbook—Fundamentals. Atlanta: ASHRAE.

Barrett, J.R. 2000. Mycotoxins: Or molds and maladies. *Environmental Health Perspectives* 108(1).

Bailey, J., and G.H. Hall. 2006. Fact sheet on controlling mold growth on window surfaces. Mold Services Group—A Division of GHH Engineering Ltd. http://moldservices-group.com/windowmold.asp. Date accessed: May 14, 2006.

Curcija, D., and W.P. Goss. 1998. The "Variable-h" model for improved prediction of surface temperatures in fenestration systems. Draft, June 1998, University of Massachusetts Report.

Dalton, L.W. 2004. Today's materials favor mold growth. *Chemical and Engineering News; Science & Technology* 82(7):60–61.

Dearborn, D.G., I Yike, W.G. Sorenson, M.J. Miller, and R.A. Etzel. Overview of investigations into pulmonary haemorrhage among infants in Cleveland, Ohio. *Environmental Health Perspectives Supplements* 107(S3).

EPA. 2001. Mold recommendation in schools and commercial buildings. U.S. Environmental Protection Agency, Office of Air and Radiation, Indoor Environments Division.

EPA. 2002. A brief guide to mold, moisture and your home. US Environmental Protection Agency, Office of Air and Radiation, Indoor Environments Division.

EPA. 2006a. Mold web course. Last updated March 13, 2006.US Environmental Protection Agency.

EPA. 2006b. Mold resources. www.epa.gov/mold/moldresources.html. Date accessed: May 14, 2006. US Environmental Protection Agency.

Fisk, W.J., Q.L. Gomez, and M.J. Mendell. 2006. Meta-analyses of the associations of respiratory health effects with dampness and mold in homes. Environmental Energy Technologies Division, Indoor Environmental Department, Lawrence Berkeley National Laboratory.

Godish, T., 2002. Indoor environmental notebook, everything you wanted to know about indoor air pollution and more. Ball State University, Department of Natural Resources and Environmental Management, Date accessed: May 14, 2006.

Grant, C., C.A. Hunter, B. Flannigan, and A.F. Bravery. 1989. Moisture requirements of moulds isolated from domestic dwellings. *International Biodeterioration* 25(4):259–84.

IOM. 2004. Damp indoor spaces and health. The National Academies, Washington: The National Academies of Sciences. Institute of Medicine.

Kansal, V. 2006. The formation and run-off of condensate on a vertical glass surface: an experimental study, MASc thesis. Department of Mechanical Engineering, University of Waterloo, https://uwspace.uwaterloo.ca/handle/10012/2695.

Kuhn, R.C. 2005. Prevalence and airborne spore levels of *Stachybotrys spp.* in 200 houses with water incursions in Houston, Texas. *Canadian Journal of Microbiology* 55:25–28.

Lstiburek, J. 2002. Relative humidity. Research report—0203, 2008 Building Science Press, April 23, 2002.

McNeel, S.V., and R.A. Kreutzer. 1996. Fungi & indoor air quality. *Health & Environment Digest* 10(2):9–12.

Morrell, J.J. 2002. Wood-based building components: What have we learned? *International Biodeterioration & Biodegradation* 49(4):253–58.

NRCan. 2005. 2003 survey of household energy use (SHEU) summary report, December 2005. Natural Resources

Canada, Energy Publications, Office of Energy Efficiency, Her Majesty the Queen in Right of Canada. 2006.

Pasanen, A.L., H. Heinonen-Tanski, P. Kalliokoski, and M.J. Jantunen. 1992. Fungal microcolonies on indoor surfaces—An explanation for the base-level fungal spore counts in indoor air. *Atmospheric Environment* 26B(1):117–20.

Post, N.M. 1999. Containing noxious mold. *Engineering News Record* 242(17):32.

Reilly, S. 1994. Spacer effects on edge-of-glass and frame heat transfer. *ASHRAE Transactions* 100(1):1718–23.

Sullivan, H.F., J.L. Wright, and R.A. Fraser. 1996. Overview of a project to determine the surface temperatures of insulated glazing units: thermographic measurement and 2-D simulation, *ASHRAE Transactions* 102(2):516–522.

Underwood, A. 2000. A hidden health hazard. *Newsweek Magazine* 136(23):74. New York.

Vaisala O. 2005. *Vaisala HUMICAP Humidity and Temperature Transmitter Series HMT330 User's Guide*. Vaisala©.

Wang, G-S., K.Y. Yang, and R.P. Perng. 2001. Life-threatening hypersensitivity pneumonitis induced by docetaxel (taxotere). *British Journal of Cancer* 85(9):1247–50.

White, C.W., and M.H. Kuehl. 2002. The role of construction textiles in indoor environmental pollution. *Journal of Industrial Textiles* 32(1).

Wright, J.L. 1998. A simplified numerical method for assessing the condensation resistance of windows. *ASHRAE Transactions* 104(1)1222–29.

Wright, J.L., and A.G. McGowan. 2003. A comparison of calculated and measured indoor-side window temperature profiles. *ASHRAE Transactions* 109(2):857–70.

Wright, J.L., and H.F. Sullivan. 1989. Thermal resistance measurement of glazing system edge-seals and seal materials using a guarded heater plate apparatus. *ASHRAE Transactions* 95(2)766–71.

Wright, J.L., P.F. de Abreu, R.A. Fraser, and H.F. Sullivan. Heat transfer in glazing system edge-seals: Calculations regarding various design options, *ASHRAE Transactions* 100(1):1705–17.

Wright, J.L., and H.F. Sullivan. 1995. A two-dimensional numerical model for glazing system thermal analysis. *ASHRAE Transactions* 101(1):819–31.